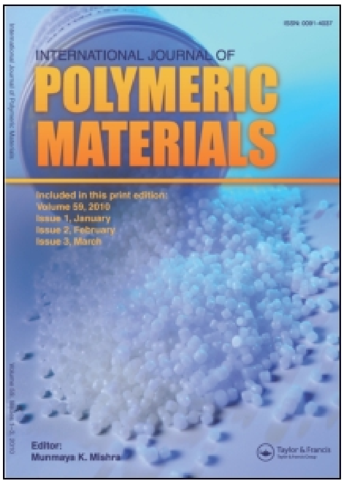

International Journal of Polymeric Materials
Publication details, including instructions for authors and subscription information:
http://www.informaworld.com/smpp/title~content=t713647664

Morphology and Rheological Properties of PE/PP Blend Fibers

Jun Han Cho[a]; Kyung Shik Choi[a]; Sang Yong Kim[a]
[a] Department of Textile Engineering, College of Engineering, Seoul National University, Seoul, Korea

To cite this Article Cho, Jun Han , Choi, Kyung Shik and Kim, Sang Yong(1993) 'Morphology and Rheological Properties of PE/PP Blend Fibers', International Journal of Polymeric Materials, 21: 1, 19 — 29
To link to this Article: DOI: 10.1080/00914039308048508
URL: http://dx.doi.org/10.1080/00914039308048508

Intern. J. Polymeric Mater., 1993, Vol. 21, pp. 19–29
Reprints available directly from the publisher
Photocopying permitted by license only

Printed in Malaysia

Morphology and Rheological Properties of PE/PP Blend Fibers

JUN HAN CHO, KYUNG SHIK CHOI and SANG YONG KIM

Department of Textile Engineering, College of Engineering, Seoul National University, Seoul 151-742, Korea

Blends of high density polyethylene (HDPE) and polypropylene (PP) were prepared by the melt mixing method. The morphology and the rheological properties of extrudates were measured and related with the physical properties of the melt spun fibers, such as X-ray diffraction patterns, tensile properties, and birefringence.

From the SEM photographs of the fractured surfaces, it can be seen that PP forms a continuous phase in blends of 25% and 50% of HDPE, while HDPE formed in a 75% blend. In all cases, the discrete phases were finely distributed. The viscosity and the melt elasticity of HDPE were higher than those of PP and those of HDPE/PP blends were intermediate. The first normal stress difference of the extrudates increased with the increase of HDPE content, and thus the birefingence and the initial modulus of the spun fibers did with the HDPE content. However, the crystalline orientation did not show any dependence on the composition. Tenacity showed a deviation from linearity due to the incompatibility.

KEY WORDS PE/PP blend fibers, morphology, rheology.

INTRODUCTION

There may be two approaches for the modification of the polymer characteristics. One is the chemical method to search for polymers having new chemical structure or texture, and the other is the blending of existing polymers.

Few papers have been published concerning the blends of crystalline polymers, but experiments on the blends of PE and PP are carried out extensively due to their high impact strength and low temperature toughness.

Robertson and Paul[1] reported that the modulus and strength of the blends are nearly monotonic functions of blend composition. However, Noel and Carley[2] showed that tensile strength and modulus pass through maxima at PE composition of 10%.

Lovinger and Williams[3] confirmed that maximization of tensile modulus of the blends containing around 80% PP is due to the profusion of the intercrystalline links introduced by PE.

Rheological properties of PP/PE blends were studied by Plochocki,[4,5] who showed that processability became feasible by the addition of PE. Noel and Carley[2] fitted the shear rate and shear stress data from the capillary rheometer to the Ellis model, with a maximum relative error of 5%.

Alle and Lyngaae-Jorgensen[6,7] measured the shear viscosity and shear rate at various temperatures and reported that the viscosities of the blends are located between those of the two constituent polymers.

In this paper, relationships of the phase distribution morphology, rheological properties, and the melt spinning of HDPE/PP blend fibers will be developed. HDPE and PP were blended by the melt mixing method and fibers were spun at various blend ratios. The morphology and rheological properties for the blend melts and physical properties of the blend fibers were measured, and the relation between their results will be discussed.

EXPERIMENTAL

1. Material

Chips of Polyethylene and Polypropylene manufactured at DaeHan Petro-Chemical Co. Ltd. were used for the experiments. Their material specifications are listed in Table I.

2. Blending and Melt Spinning

Chips of PE and PP were melt mixed in a single screw extruder at 210°C. The mixing ratios used are shown in Table II. Melt spinning conditions for this experiment are listed in Table III. The spun fibers were wet drawn to a draw ratio of 2 at 60°C and a draw ratio of 4 at 90°C.

TABLE I

Grade and properties of PP and HDPE

	Grade	MI (g/10 min)	Density (g/cc)	m.p. (°C)
PP	5016H	15	0.90	163
HDPE	E308	0.8	0.956	129

TABLE II

Sample code and composition of HDPE/PP blends

Sample code	Composition (Vol. %)
HDPE/PP = 0/100	100% Polypropylene
25/75	25% Polyethylene and 75% Polypropylene
50/50	50% Polyethylene and 50% Polypropylene
75/25	75% Polyethylene and 25% Polypropylene
100/0	100% Polyethylene

TABLE III

Operating conditions of melt spinning tester

Specification	Condition
Screw speed	3.5–4 rpm
Gear pump speed	11 rpm
Extrusion rate	3.3 cc/min
Nozzle length (L)	10 mm
Nozzle diameter (D)	1 mm
Apparent shear rate	555 sec^{-1}
Take-up speed	85 m/min

3. Rheological Peoperties

A Rheometrics Dynamic Spectrometer (model 7700) was used for the measurement of viscosity and melt elasticity at low shear rates. For the higher shear rates, a capillary rheometer (Instron model 3210) was used.

4. Morphology and Physical Properties

SEM: SEM (Akashi ISI-DS 130) was ued to observe the morphology of extrudates at the fractured surfaces. Fractured surfaces were prepared in liquid nitrogen and the surfaces were vacuum coated with a thin layer of gold.

WAXS: Crystalline orientations of the drawn fibers were measured with Rigaku D/Max IIIA. Nickel-filtered Cu-Kα (35 kV-20 mA) radiation was used.

Birefringence: The retardation of white light was measured by a polarizing microscope (Leitz Metalloplan) and the birefringence of the drawn fibers was calculated by dividing the retardations by the fibers' diameter.

Tensile properties: Initial modulus and tensile strength were measured by using an Instron (model A1020). Gage length was 10 cm and cross-head speed was 20 cm/min.

RESULTS AND DISCUSSION

1. Morphology and Rheological Properties

Figure 1 shows the fractured surfaces of the extrudates observed by SEM. Continuous phases of PP can be seen for the samples of blend ratios 25/75 and 50/50. Sizes of discrete islands of PP at the composition of 75/25 are smaller than those of PE at 25/75.

Figure 2 shows the size distribution of the discrete islands at various blend ratios. The range of sizes is from 0.4 to 2 μm. The sizes of these blends are smaller than those of PP/Nylon 6 blend (50 μm) at the blend ratio 25/75 and are similar to those of PP/PS blends at 30/70, which is 2 μm.

Figures 3 and 4 are the rheological properties of PE/PP blends. The steady shear

(a)

(b)

(c)

(d)

(e)

FIGURE 1 SEM photomicrographs of extrudates of HDPE/PP blends. (HDPE/PP) (a) 0/100, (b) 27/75, (c) 50/50, (d) 75/25, (e) 100/0.

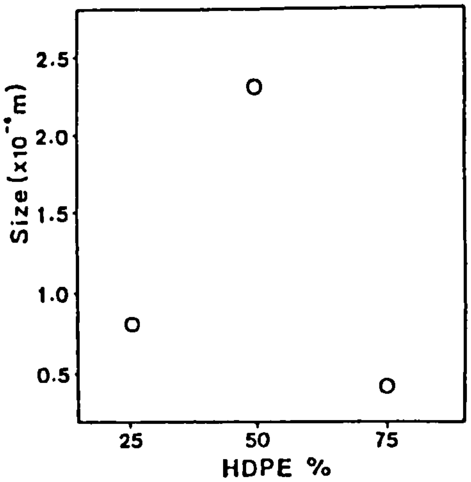

FIGURE 2 Size of the discrete islands of HDPE/PP blends.

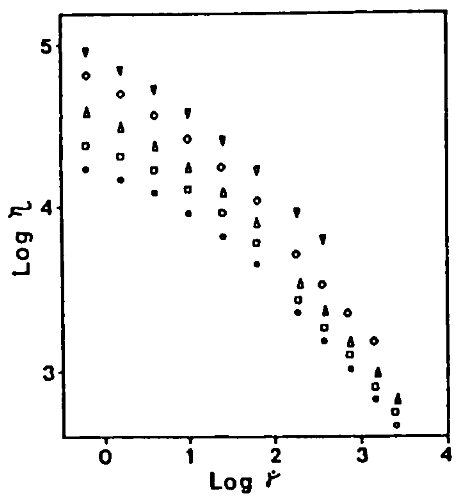

FIGURE 3 Viscosity (η)-shear rate ($\dot{\gamma}$) relation of the extrudates of HDPE/PP blends. ○: PP, □: 25/75, △: 50/50, ◇: 75/25, ▽: HDPE.

flow properties were obtained from the dynamic shear properties by the following Cox-Merz law[8,9] and Launs law.[9,10]

$$\eta(\gamma) = |\eta^*(\omega)|_{\omega=\dot{\gamma}} = [\eta'(\omega)^2 + \eta''(\omega)^2]^{1/2}_{\omega=\dot{\gamma}} \tag{1}$$

$$\Psi_1(\dot{\gamma}) = \frac{2G'}{\omega^2}\left[1 + \left(\frac{G'}{G''}\right)^2\right]^{0.7}\Bigg|_{\omega=\dot{\gamma}} \tag{2}$$

where $\dot{\gamma}$ and ω are shear rate and frequency, respectively, η is the shear viscosity, η^* the complex viscosity, η' and η'' are the real and imaginary parts of η^*, re-

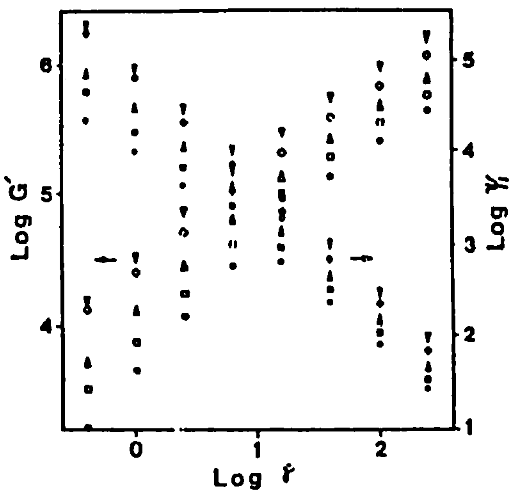

FIGURE 4 Storage modulus (G') and principal normal stress difference function (ψ_1) vs. shear rate ($\dot{\gamma}$). Symbols are the same as in Figure 3. (Filled symbols: Log ψ_1, empty symbols: Log G').

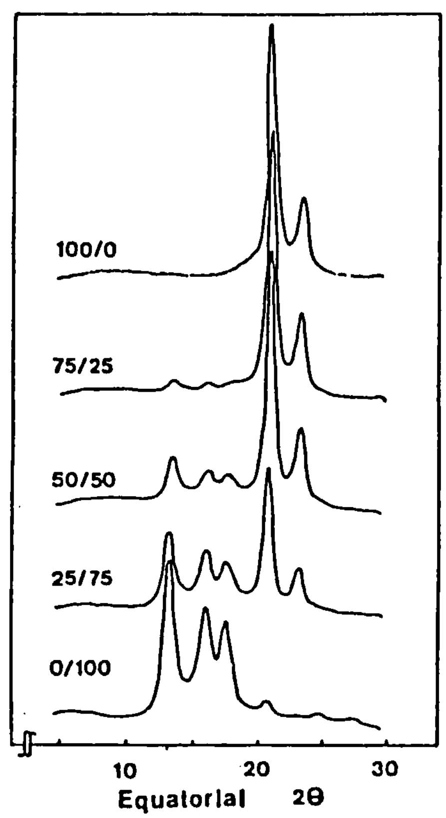

FIGURE 5 Diffractometer scans for HDPE/PP blends.

TABLE IV

Hermans-Stein orientation factors f_a, f_b and f_c for crystalline phase of HDPE in blends

HDPE %	Orientation factors		
	f_a	f_b	f_c
0	—	—	—
25	−0.473	−0.470	0.943
50	−0.485	−0.486	0.971
75	−0.483	−0.481	0.964
100	−0.475	−0.473	0.948

TABLE V

Hermans-Stein orientation factors f_a, f_b and f_c for crystalline phase of PP in blends

HDPE %	Orientation factors		
	f_a	f_b	f_c
0	−0.477	−0.480	0.957
25	−0.457	−0.458	0.915
50	−0.472	−0.473	0.945
75	−0.473	−0.474	0.947
100	—	—	—

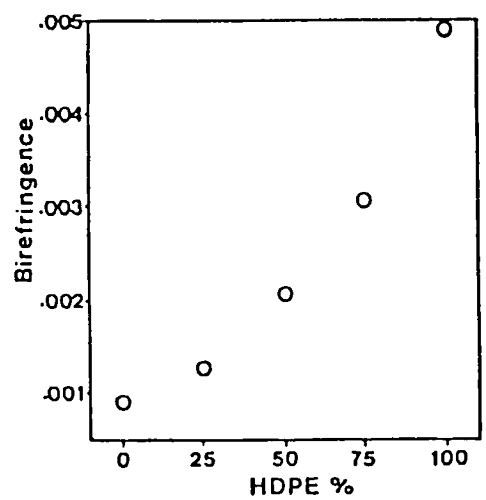

FIGURE 6 Birefringence of the drawn HDPE/PP blend filaments (draw ratio: 8).

spectively. Ψ_1 is the first normal stress difference and G' and G'' are the storage and loss moduli, respectively.

Data at the high shear rates ($\dot{\gamma} > 100\ s^{-1}$) were measured by using a capillary rheometer. The relation between the two rheometers, the RDS and capillary rheometer, were also confirmed by Liang and White[11] and Min and White,[12] that is,

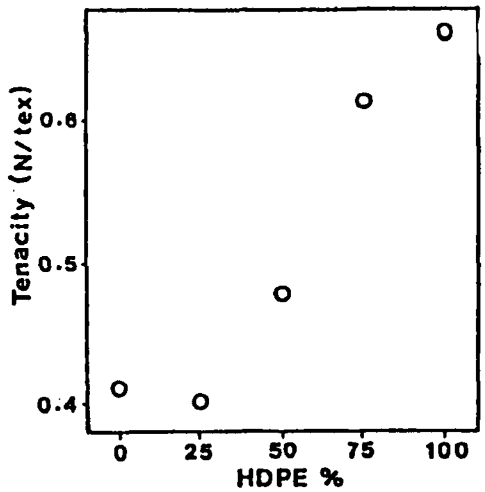

FIGURE 7 Tenacity of the drawn HDPE/PP blend filaments.

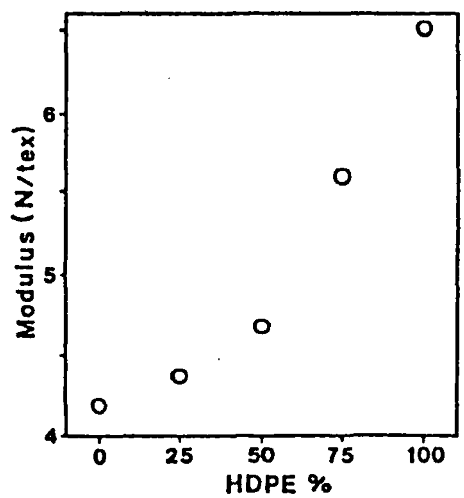

FIGURE 8 Initial modulus of the drawn HDPE/PP blend filaments.

the sizes of the discrete islands are very small compared with the capillary and nozzle sizes.

Viscosities of PE at the initial shear rates are very high compared with those of PP. Blend viscosities are between those of the two homoblends as reported by others, such as Lingaae-Jorgensen[6,7] and Valenza.[13] Figure 4 shows the variation of storage modulus and the first normal stress difference with respect to the shear rates. Melt elasticity of PE is higher than that of PP, and for the blends, it increases with the increase of HDPE content.

2. Physical Properties of Melt Spun Fibers

Figure 5 shows the WAXS patterns of PE, PP and their blend fibers. PE appeared to have the same diffraction patterns as those of Min and White's results.[12] Diffraction patterns of PP were the same as those of Liang and White.[11] Crystal structures of PE and PP are tetrahedral and monoclinic, respectively. Characteristic peaks of PP were at 13.8° and 16.6° corresponding to (110) and (040) planes, respectively. For PE, characteristic peaks are at 21.2° and 23.6° corresponding to (110) and (200) planes, respectively. In the blends, these peaks were superimposed.

Tables IV and V show the crystalline orientations of PE and PP in the blends measured for the drawn specimens of draw ratio 8. Orientation factors (f_j) are shown as follows:

$$f_j = \frac{3\,\overline{\cos^2\phi} - 1}{2} \tag{3}$$

where ϕ_j is the angle between the fiber axis and the crystal j-axis. For PP, the Wilchinsky method[11,14,15] was used to calculate the orientation factors. For example, the b-axis orientation factor was obtained from the peak of (040) planes and the c-axis factor was calculated by the following Wilchinsky formula:

$$\overline{\cos^2\phi_c} = 1 - 1.099\,\overline{\cos^2\phi_{110}} - 0.901\,\overline{\cos^2\phi_{040}} \tag{4}$$

where ϕ_{110} and ϕ_{040} are the angles between the fiber axis and (110) and (040) planes, respectively.

In the case of PE, the a-axis orientation factor f_a can be obtained from the peak of (200) plane and f_b can be calculated by the Stein formula[12,16] as below:

$$\overline{\cos^2\phi_b} = \frac{\overline{\cos^2\phi_{110}} - 0.308\,\overline{\cos^2\phi_{200}}}{0.692} \tag{5}$$

where ϕ_{110} and ϕ_{200} are the angles between the fiber axis and (110) and (200) planes, respectively. The remaining orientation factor f_c can be obtained from the following relation:

$$f_a + f_b + f_c = 0 \tag{6}$$

The angle between the a- and c-axes is 99.3° for the PP of the monoclinic system; thus by assuming the hypothetical a'-axis perpendicular to the b and c planes, Equation (6) can be used to calculate the orientation factors.[14]

By comparing Tables IV and V, it can be said that the crystalline orientation does not depend on the blend ratio. But the PE orientations in the blends were shown to be slightly higher than the PP orientation, probably due to the fact that the more viscous PE withstands the higher stress and impedes the relaxation of extended chains.

Figure 6 shows the relation between the birefringence of drawn fibers vs. blend ratios. The birefringence of PE is higher than that of PP and the blends, and the birefringence increases monotonically with the blend ratios between the two limits.

Figures 7 and 8 show the tenacity and the initial modulus of drawn fibers, respectively. Initial modulus is a monotonic function of the blend ratio of PE, deviating from linearity due to the incompatibility behavior. Tenacity also deviates from linearity and has a minimum value at the blend ratio 25/75, probably due to the earlier fracture of the specimen causing a larger cross-sectional area. Lovinger[3] also reported the lowering of the true strength at the same blend ratio.

Birefringence is the result of both the crystalline and amorphous orientations and this is related to bulk physical properties. As shown in Figures 7 and 8, the modulus can be seen to be proportional to the birefringence.

CONCLUSIONS

HDPE and PP were melt blended and spun at 210°C. PP forms a continuous phase in the blends of 25/75 and 50/50 while HDPE does in 75/25. In all cases the discrete phases were finely distributed. The viscosity and melt elasticity of HDPE were higher than those of PP and those of HDPE/PP blends were intermediate. The first normal stress difference increases with increase of HDPE content and thus the birefringence and the initial modulus of the spun fibers do likewise. Moreover, the crystalline orientation did not show any dependence on the compositions. Tenacity shows a deviation from linearity due to the incompatibility.

References

1. R. E. Robertson and D. R. Paul, Stress-Strain Behavior of Polyolefin Blends, *J. Appl. Polym. Sci.*, **17**, 579–2595 (1973).
2. O. F. Noel and J. F. Carley, Properties of Polypropylene-Polyethylene Blends, *Polym. Eng. Sci.*, **15**, 117–126 (1975).
3. A. J. Lovinger and M. L. Williams, Tensile Properties and Morphology of Blends of Polyethylene and Polypropylene, *J. Appl. Polym. Sci.*, **25**, 1703–1713 (1980).
4. A. Plochocki, On the Rheology of Molten Binary Blends of Polyolefins. X. Homogeneity and High Shear Melt Flow of Polypropylene-Polyethylene Blends, *J. Appl. Polym. Sci.*, **16**, 987–1008 (1972).
5. A. Plochocki, "Polymer Blends," ed. by D. R. Paul, S. Newman, Vol. II, Academic, New York, Chap. 21 (1978).
6. N. Alle and J. Lyngaae-Jorgensen, Polypropylene and Polyethylene Blends. I. Flow Behavior in Capillaries, *Rheol. Acta*, **19**, 94–103 (1980).
7. N. Alle and J. Lyngaae-Jorgensen, Polypropylene Polyethylene Blends. II. The Relationship Between Rheology and Morphology in Capillary Flow, *Rheol. Acta*, **19**, 104–110 (1980).
8. W. P. Cox and E. H. Merz, Correlation of Dynamic and Steady Flow Properties, *J. Polym. Sci.*, **28**, 619–622 (1958).
9. R. B. Bird, R. C. Armstrong and O. Hassager, "Dynamics of Polymeric Liquids," J. Wiley & Sons, New York, Chap. 3 (1987).
10. H. M. Laun, Prediction of Elastic Strains of Polymer Melts in Shear and Elongation, *J. Rheol.*, **30**, 459–501 (1986).
11. B. Liang, J. L. White and J. E. Spruiell, Polypropylene/Nylon 6 Blends: Phase Distribution Morphology, Rheological Measurements, and Structural Development in Melt Spinning, *J. Appl. Polym. Sci.*, **28**, 2011–2032 (1983).
12. K. Min, J. L. White and J. F. Fellers, High Density Polyethylene/Polystyrene Blends: Phase Distribution Morphology, Rheological Measurements, Extrusion, and Melt Spinning Behavior, *J. Appl. Polym. Sci.*, **29**, 2117–2142 (1984).
13. A. Valenza, F. P. La Mantia and D. Acierno, Rheological Characteristics of Blends of Isotactic Polypropylene with High Density Polyethylene, *Eur. Polym. J.*, **20**, 727–731 (1984).

14. Z. W. Wilchinsky, Measurement of Orientation in Polypropylene Film, *J. Appl. Phys.*, **31**, 1969–1972 (1960).
15. H. P. Nadella, H. M. Henson, J. E. Spruiell and J. L. White, Melt Spinning of Isotactic Polypropylene: Structure Development and Relationship to Mechanical Properties, *J. Appl. Polym. Sci.*, **21**, 3003–3022 (1977).
16. R. S. Stein, The X-ray Diffraction, Birefringence, and Infrared Dichroism of Stretched Polyethylene. II. Generalized Uniaxial Crystal Orientation, *J. Polym. Sci.*, **31**, 327–334 (1958).